Monthly Notices
of the
ROYAL ASTRONOMICAL SOCIETY

MNRAS **458,** 2596–2603 (2016)
Advance Access publication 2016 March 07

doi:10.1093/mnras/stw531

High-velocity stars from the interaction of a globular cluster and a massive black hole binary

G. Fragione★ and R. Capuzzo-Dolcetta

Department of Physics, Sapienza University of Rome, Piazzale Aldo Moro, 2, I-00185 Roma, Italy

Accepted 2016 March 2. Received 2016 March 2; in original form 2015 November 16

ABSTRACT

High-velocity stars are usually thought to be the dynamical product of the interaction of binary systems with supermassive black holes. In this paper, we investigate a particular mechanism of production of high-velocity stars as due to the close interaction between a massive and orbitally decayed globular cluster and a supermassive black hole binary. The high velocity acquired by some stars of the cluster comes from combined effect of extraction of their gravitational binding energy and from the slingshot due to the interaction with the black hole binary. After the close interaction, stars could reach a velocity sufficient to travel in the halo and even overcome the galactic potential well, while some of them are just stripped from the globular cluster and start orbiting around the galactic centre.

Key words: stars: kinematics and dynamics – galaxies: haloes – galaxies: nuclei – galaxies: star clusters: general.

1 INTRODUCTION

Massive black holes (BHs) are present in most of the galactic nuclei over the whole Hubble sequence and are recognized as fundamental building blocks in models of galaxy formation and evolution (Kormendy & Ho 2013). According to the standard cosmological model, the formation of structures involves mergers of galaxies, which follow the hierarchical growth of their parent dark matter haloes (Mayer et al. 2007; Roškar et al. 2015). Galaxies may experience multiple mergers during their lifetime and, if more than one contain a massive BH, the formation of a black hole binary (BHB) is a natural consequence of the hierarchical paradigm (Volonteri, Haardt & Madau 2003).

How long BHBs survive and whether they eventually merge are key questions in high-energy and extragalactic astronomy. Through the loss of their orbital energy and angular momentum, two massive BHs become gravitationally bound until their final merging. BHBs are thought to undergo several dynamical stages before their coalescence (Begelman, Blandford & Rees 1980; Yu 2002). The first stage is the dynamical friction stage, during which each BH inspirals independently towards the centre of the common gravitational potential on the Chandrasekhar time-scale (Chandrasekhar 1943). During the second stage, usually referred to as non-hard binary stage, the BHs speeds increase, while their orbital period shortens, because more and more stars in the galactic nuclear core are scattered off the system through three-body interactions. At the same time, the energy loss due to dynamical friction becomes less efficient. The successive stage, labelled hard binary stage, begins when the orbital separation is of the order of (Quinlan 1996)

$$a_h = 2.8 \left(\frac{m_{\rm BH,2}}{10^8\,{\rm M}_\odot}\right)\left(\frac{200\ {\rm km\ s^{-1}}}{\sigma_c}\right)^2\ {\rm pc}\,, \quad (1)$$

where σ_c is the one-dimensional velocity dispersion, while $m_{\rm BH,2}$ is the mass of the lighter BH. Hard BHBs lose energy mainly by three-body slingshot effect with stars passing in their vicinity, which can be expelled after one or more encounters. The duration of this stage depends on the loss-cone refill of the scattered stars and the BH binary may stall at parsec scale (Merritt & Milosavljević 2005; Perets & Alexander 2008). The last stage is characterized by the energy loss due to gravitational radiation. A BHB will coalesce within the time (Peters 1964)

$$t_{\rm coal} \sim \frac{5.8\, m_{\rm BH,1}^2 \times 10^6}{m_{\rm BH,2}\, M}\left(\frac{a}{0.01\ {\rm pc}}\right)^4\left(\frac{10^8\,{\rm M}_\odot}{m_{\rm BH,1}}\right)^3, \quad (2)$$

where $m_{\rm BH,1}$ is the mass of the heavier BH and $M = m_{\rm BH,1} + m_{\rm BH,2}$ is the total BHB mass.

Many galaxies show nucleated central regions, the so-called nuclear star clusters (NSCs), which are among the densest stellar populations observed in the Universe (Carollo et al. 1997; Côté et al. 2006; Turner et al. 2012). Two different processes are thought to give birth to NSCs. The first mechanism, which involve radial gas inflow into the galactic centre and requires efficient dissipation processes to work, predicts that NSCs consist mostly of stars formed locally (Loose, Kruegel & Tutukov 1982; Schinnerer et al. 2006, 2008). The second mechanism suggests massive stellar clusters, such as globular clusters (GCs), spiral into the centre of the galaxy where merge to form a dense nucleus (Tremaine, Ostriker & Spitzer

★E-mail: giacomo.fragione@uniroma1.it

1975; Capuzzo-Dolcetta 1993; Capuzzo-Dolcetta & Miocchi 2008; Antonini 2013). In the latter scenario, due to strong interactions with the central massive BH along the process of GC infall in the galactic centre, many stars, formerly belonging to the cluster, can be accelerated to high velocities and ejected in jets from the inner galactic regions (Capuzzo-Dolcetta & Fragione 2015).

High-velocity stars have been observed in the Galactic halo. Several physical mechanisms may be responsible for such high velocities like three-body interactions involving the massive BH in the Galactic Centre, or kicks due to supernova explosions. High-velocity stars can be divided in two different categories, i.e. runaway stars (RS) and hypervelocity stars (HVSs).

RSs, historically defined in the context of O and B stars (Humason & Zwicky 1947), are Galactic halo stars with peculiar motions higher than 40 km s^{-1}. Such young massive stars are not expected to be present far from star-forming regions and are thought to have travelled far from their birthplace. RSs are produced in binary systems or thanks to the velocity kick due the supernova explosion of the former companion (Blaauw 1961; Portegies Zwart 2000) or thanks to dynamical three- or four-body interactions (Poveda, Ruiz & Allen 1967; Perets & Subr 2012). Observations show that, likely, both these ejection mechanisms operate in nature (Hoogerwerf, de Bruijne & de Zeeuw 2001), but, in any case, RSs velocities are below the Galaxy escape velocity.

HVSs are stars escaping the Galaxy (Brown 2015). Hills (1988) was the first to predict theoretically their existence, while Brown et al. (2005) serendipitously discovered the first HVS in the outer halo. Hills' mechanism involves the tidal breakup of a binary passing close to a massive BH. Moreover, Hills' scenario predicts the existence of a population of stars orbiting in the inner Galactic regions around the central BH (Ginsburg & Loeb 2006; Perets, Hopman & Alexander 2007). Other mechanisms have, also, been proposed to explain the existence of HVSs (Brown 2015), as the interaction of an Super Massive Black Hole Binary (SMBHB) with a single star (Sesana, Haardt & Madau 2006), the arrival from another nearby galaxy (Brown et al. 2010) and the supernova explosion in a close binary (Zubovas, Wynn & Gualandris 2013).

Since high-velocity stars production mechanisms involve different astrophysical phenomena, it would be possible to infer information about different pieces of physics, as the physics of regions near massive BHs (O'Leary & Loeb 2008; Lu, Zhang & Yu 2010; Zhang, Lu & Yu 2010), the Galaxy gravitational potential and its dark matter component (Gnedin et al. 2005; Yu & Madau 2007; Perets et al. 2009).

Observations of high-velocity and hypervelocity objects have usually been limited to high-mass, early-type, stars, due to obvious observational bias (Brown et al. 2010; Brown, Geller & Kenyon 2014). Nowadays, observers have started investigating low-mass high-velocity stars (Palladino et al. 2014; Zhong et al. 2014). Moreover, the European ESA satellite *Gaia*, along with *Gaia-ESO*, is expected to measure proper motions with an unprecedented precision, providing a larger and less biased sample. The *Gaia* mission is expected to measure proper motions of ∼100 new HVSs in our Galaxy. However, such measurements are limited in magnitude and so in distance, according to *Gaia* sensitivity. For example, 1 and 3 $M_\odot$ HVSs could be detected in the Galactic halo within ∼10 and ∼100 kpc, respectively. Therefore, these upcoming data will be useful to study high-velocity stars only in the Milky Way environment. However, extended spectroscopic surveys will lead to reliable measurements of stars radial velocities also in other galaxies. Of course, such observations are still biased towards high-luminosity, and so high mass, stars.

The aim of this paper is to investigate a particular mechanism of production of high-velocity stars which involves a GC and an SMBHB. Actually, when, due to dynamical friction, the orbit of a GC approaches closely a BHB in the centre of its host galaxy, some of its stars are stripped from the cluster and are ejected with high velocities. For the test cases of this paper, we assumed a total SMBHB mass $M = 10^8$ $M_\odot$, with the scope of a clear comprehension of the efficiency of this physical mechanism and of making comparison with our previous results obtained in the case of a single massive BH (Capuzzo-Dolcetta & Fragione 2015). Moreover, we performed the same set of simulations for $M = 10^7$ $M_\odot$, to study the effect of the total mass of the BHB on the results.

The paper is organized as follows: in Section 2, we describe our approach to the study of the consequences of the GC–BHB interaction; in Section 3, the results of our scattering experiments are presented and discussed. Finally, in Section 4 we draw the conclusions.

2 METHOD

Our scattering experiments refer to the interaction of three different components: an SMBHB, a GC and, a star belonging to the GC. In our simulations the SMBHB centre of mass sits initially in the origin of the reference frame, while the GC follows a relatively close elliptical orbit around the SMBHB. The assumption of close distance to the BHB is motivated by the fact that the GC is supposedly orbitally decayed by dynamical friction braking suffered along its motion in the galaxy.

The influence length-scale of the BHB is likely larger than the influence radius of a single BH of mass equal to the BHB total mass, due to strong tidal torque. Assuming (as we do in this paper) a total BH mass $M = 10^8$ $M_\odot$, the influence radius of the single BH of that mass is $r_{\rm inf} \simeq 12.5$ pc, larger than the assumed value of the radius ($r_0 = 10$ pc, see choice of parameters below) of the GC reference circular orbit. This makes reliable the assumption of neglecting the galactic background potential in our scattering experiments, unless exceedingly cuspy galactic background matter densities are considered. Neglecting the external potential implies also neglecting dynamical friction on the GC motion, thing that leads to a slight underestimate of the encounter effect on the test star, which would actually encounter the BHB at a shorter distance.

The SMBHB was assumed to revolve on an initial circular orbit. The distance between the BHs is $r_{\rm BHB} = r_{{\rm BH},1,c} + r_{{\rm BH},2,c} = a_h$. Therefore, the heavier BH has initial conditions given by

$$r_{{\rm BH},1,c} = \frac{m_{\rm BH,2}}{M} a_h; \quad v_{{\rm BH},1,c} = \sqrt{\frac{G}{M a_h}} m_{\rm BH,2}, \tag{3}$$

while for the lighter BH they are

$$r_{{\rm BH},2,c} = \frac{m_{\rm BH,1}}{M} a_h; \quad v_{{\rm BH},2,c} = \sqrt{\frac{G}{M a_h}} m_{\rm BH,1}, \tag{4}$$

where $r_{{\rm BH},1,c}$ and $r_{{\rm BH},2,c}$ are the radii of the circular orbits around their centre of mass.

The orbital energy (per unit mass) of the GC on a circular orbit of radius $r_{\rm c}$ around the BHB centre of mass (neglecting the potential of the stellar background), is

$$E_{\rm c} \equiv \frac{1}{2} v_{\rm c}^2 - \frac{GM}{r_{\rm c}} = -\frac{1}{2} \frac{GM}{r_{\rm c}}, \tag{5}$$

where $v_{\rm c} = \sqrt{GM/r_{\rm c}}$ is the circular velocity. Thereafter, taking into account that the angular momentum (per unit mass) of the GC on

Table 1. The values of the BHB mass ratio ν and of the radius of the initial binary circular orbit $r_{\rm BHB}$.

ν	$r_{\rm BHB}$ (pc)
1/20	0.16
1/10	0.31
1/5	0.62
1/4	0.78
1/3	1.04
1/2	1.56

the circular orbit is $L_{\rm c} = \sqrt{GMr_{\rm c}}$, the pericentre ($r_-$) and apocentre ($r_+$) distances of the GC on orbits of given energy ($E_{\rm c}$) and angular momentum $0 \leq L \leq L_{\rm c}$, are given by

$$r_\pm = r_{\rm c}\left[1 \pm \sqrt{1-\left(\frac{L}{L_{\rm c}}\right)^2}\right]. \quad (6)$$

Therefore, by varying the ratio $\alpha = (L/L_{\rm c})^2$, we can compare the circular orbit with a set of orbits at same energy, but different eccentricity

$$e = \frac{r_+ - r_-}{r_- + r_+} = \sqrt{1-\alpha}. \quad (7)$$

Furthermore, in our simulations, the GC is assumed to have a Plummer (1911) mass profile

$$M(r) = M_{\rm GC}\frac{r^3}{(r^2+b^2)^{3/2}}, \quad (8)$$

where $M_{\rm GC}$ is the total GC mass and b its core radius. The test star is assumed on an initial circular orbit inside the GC Hill's sphere of influence.

The Cartesian reference frame has been chosen with the x-axis along the line connecting the GC to the SMBHB centre of mass and y-axis such that the (x, y) frame is equiverse to the GC orbital revolution.

To summarize, the values of the relevant initial parameters have been set as follows (see also Table 1):

(i) the total mass of the SMBHB is $M = 10^8$ M$_\odot$;
(ii) the binary mass ratio $\nu = m_{\rm BH,\,2}/M$ assumes the values of 1/2, 1/3, 1/4, 1/5, 1/10, and 1/20;
(iii) the radius, $r_{\rm BHB}$, of the SMBHB initial circular orbit is set equal to a_h;
(iv) the initial phase, Ψ, of the BHB orbit is randomly generated;
(v) the GC mass, $M_{\rm GC}$, is fixed to 10^6 M$_\odot$;
(vi) the GC core radius, b, is set to 0.2 pc;
(vii) the radius of the GC reference circular orbit is $r_0 = 10$ pc;
(viii) the GC orbital eccentricity ranges from $e = 0.71$ ($\alpha = 0.5$) to $e = 0.95$ ($\alpha = 0.1$) and is parametrized varying α at steps of 0.1;
(ix) the GC orbits are coplanar with the SMBHB one;
(x) the test star mass, m_*, is set equal to 1 M$_\odot$;
(xi) the test star circular orbit radii are set equal to $r_L/4$, $r_L/6$, $r_L/8$, $r_L/10$, where $r_L = r_0(M_{\rm GC}/3M)^{1/3}$ is the radius of the Hill's sphere;
(xii) the star initial position on the circular orbits is randomly generated;
(xiii) the angles θ, ϕ, ψ, which determine the orientation of the star circular orbit in the GC reference frame, are randomly generated.

The choice of the range of α, and consequently of e, towards large values of e, is justified by the fact that the efficiency of the energy transfer on the test star orbiting the GC tends to vanish at eccentricities less than ∼0.6 (see Capuzzo-Dolcetta & Fragione 2015). We stress that the role of the GC orbital eccentricity in these simulations is that of a parameter tuning the GC pericentre distance to the BHB, which is one of the actually important quantity in determining the fate of the test star after the GC–BHB encounter. Anyway, high GC eccentricities are not in contradiction with the alleged effect of circularization of dynamical friction since such a circularization does not occur on orbits which are initially eccentric enough.

The assumption of test stars revolving the GC on circular orbits, only, is not a serious limitation, as already pointed out in Capuzzo-Dolcetta & Fragione (2015). Actually, eccentric test star motions generally mimic results for circular orbits with appropriately larger semimajor axes. This was previously found by Bromley et al. (2006) in the context of binary star–Super Massive Black Hole (SMBH) encounters.

Given the above set of initial parameters, we integrated the system of differential equations of motion of the four-bodies involved (SMBHB, GC, and star)

$$\ddot{\boldsymbol{r}}_i = -G\sum_{j\neq i}\frac{m_j(\boldsymbol{r}_i - \boldsymbol{r}_j)}{|\boldsymbol{r}_i - \boldsymbol{r}_j|^3}, \quad (9)$$

with $i = 1, 2, 3, 4$, using the fully regularized algorithm of Mikkola & Aarseth (2001). The enormous range of variation of the involved masses requires indeed regularization of the interaction forces, because any not-regularized direct summation code would fail when dealing with close star–SMBHB interactions and, consequently, would carry to a huge numerical error during such close encounters. Thanks to a transformed leapfrog algorithm combined with the Bulirsch–Stoer extrapolation method (Bulirsch & Stoer 1966), the Mikkola's ARW code overcomes this problem and leads to extremely accurate integrations of the bodies trajectories (Mikkola & Tanikawa 1999a,b; Mikkola & Merritt 2006, 2008; Hellström & Mikkola 2010). Thanks to the use of the regularized algorithm, the fractional energy error is kept below 10^{-10} over the whole integration time.

3 RESULTS

In our scattering experiments the test star orbiting the GC has three possible fates after the interaction with the SMBHB: the star can (i) remain bound to the GC, but on an orbit significantly perturbed with respect to the original one, or (ii) can be captured by the SMBHB and starts orbiting around the galactic centre on precessing loops, or (iii) can be lost by the GC–SMBHB system.

The distinction among these three cases is made by computing the mechanical energy of the star with respect to the SMBHB and the GC after the scattering. If its energy with respect to the GC remains negative, the star remains bound to the GC [case (i)], while if this energy becomes positive, and contemporary the star energy with respect to the BHB is negative, the star becomes bound to the binary [case (ii)]. Finally, if both these energies are positive, the star is able to leave the SMBHB–GC system [case (iii)].

In this paper, we focus our attention on the stars ejected at high velocities after the interaction with the SMBHB, examining the role of the mass ratio and of the SMBHB orbital eccentricity.

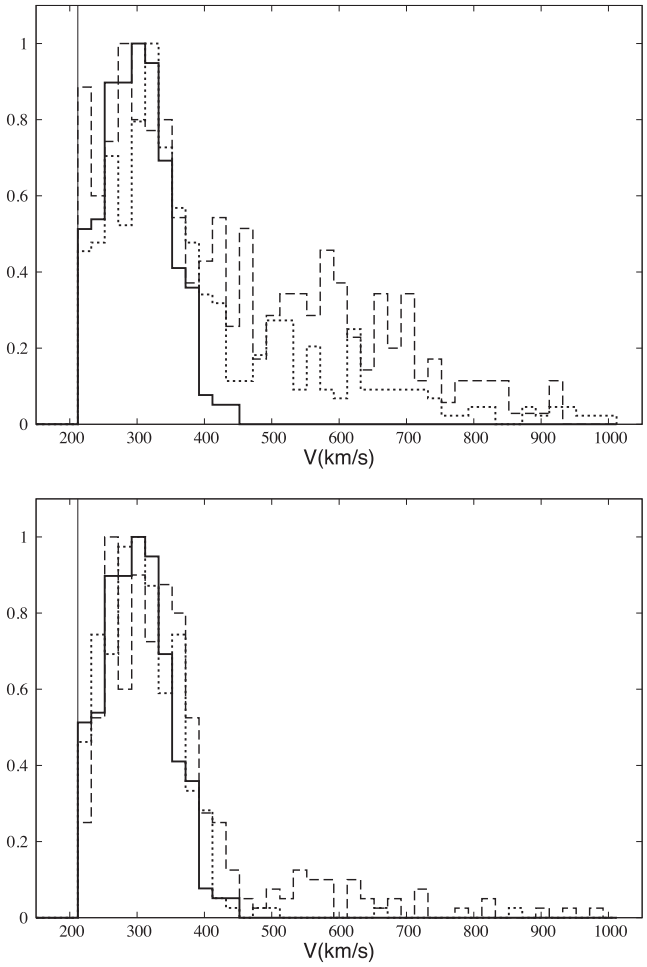

Figure 1. Comparison between the velocity distributions of escaping stars for different BH binary mass ratios and single BH ($\nu = 0$, solid line). The top panel represents the distributions for high-mass ratios ($\nu = 1/3$, dashed line, and $\nu = 1/5$, dotted line), while the bottom panel low-mass ratios ($\nu = 1/10$, dashed line, and $\nu = 1/20$, dotted line). The distributions are cut on the left side at 212 km s^{-1}, which corresponds to the escape velocity with respect to the system at 20 pc.

3.1 The role of the BHB mass ratio

Our scattering experiments allow us to derive the velocity distribution of the ejected stars. In the case of a single massive BH, the velocity distribution is narrow and peaked at small velocities, depending on the GC core radius (Capuzzo-Dolcetta & Fragione 2015). When the GC has a Plummer profile (equation 8) the initial gravitational energy, $E_{g,*}$, of the star is $\sim GM_{\rm GC}/b$ (in our simulations $b = 0.2$ pc). In this case, the velocity distribution is peaked at a lower value with respect to the case of a point-mass GC (Capuzzo-Dolcetta & Fragione 2015). Actually, the star ejection velocity depends on the initial value of $E_{g,*}$ and on the pericentre r_- of the GC orbit. Moreover, the width of the (nearly Gaussian) distribution is determined, besides by the different (randomly generated) initial position angles along the star circular orbit and other initial conditions, by the angle, γ, between the angular momentum vector of the cluster and that of the test star. Actually, if $\gamma \sim 0$ during the close interaction (i.e. near the pericentre of the GC orbit with respect to the BHB centre of mass) the ejection velocity, and the ejection probability, of the star will be higher than in cases of large values of γ ($\gg$0). Fig. 1 shows the resulting nearly Gaussian velocity distribution, for all the values of α studied, which peaks at $\sim$300 km s^{-1} in the case of single BH (solid line).

The situation changes when dealing with scattering with a BH binary. Actually, in this case the ejection velocity depends not only on $E_{g,*}$, r_p, and γ, but also on ν, and so on a_h. The generic star of an infalling GC is able to exchange energy with the binary through gravitational slingshot, which enhances its ejection velocity. On the other hand, the energy transfer makes the SMBHB shrink reducing the apocentre of its orbit. Fig. 1 shows the resulting velocity distribution for BHB for different values of ν. If the mass ratio is high (top panel), a considerably extended tail in the distribution up to $\sim$1000 km s^{-1} is produced. On the contrary, if the mass ratio is low (bottom panel), the differences between the distributions in the single and binary BH cases are not so pronounced. In particular, if $\nu \lesssim 1/20$, the velocity distributions for single and binary BHs are very similar.

Velocity distributions show that for high values of ν the fraction of ejected stars, which acquire significantly high velocities, is relevant. Actually. for $\nu \gtrsim 1/5$, the tail of the distribution extends up to $\sim$1000 km s^{-1}. Therefore, a considerable fraction of ejected stars is unbound not only with respect to the SMBHB–GC system, but also with respect to the host galaxy itself, becoming HVSs. The escape velocity (evaluated at 20 pc from the centre, as justified in Capuzzo-Dolcetta & Fragione 2015) for an elliptical galaxy, like NGC 3377 (Marconi & Hunt 2003), of total mass $M_{\rm E} = 7.81 \times 10^{10}$ M$_\odot$, is 418 km s^{-1}, while for a spiral galaxy, of total mass $M_{\rm S} = 6.60 \times 10^{11}$ M$_\odot$, it is 759 km s^{-1} (Fujita 2009). Fig. 1 shows that a non-negligible fraction of ejected stars is beyond the local escape velocity. The fate of these stars is to escape the SMBHB–GC system, to travel across the halo and eventually leave the host galaxy.

The introduction of a secondary BH, comparable in mass with the primary, leads to a peculiar distribution velocity for the stars ejected at high velocities. In principle, these distributions could be used to distinguish whether the central massive object is a single or a binary BH, in a future when data for proper motions and radial velocities will be available for galaxies whose central object(s) total mass is of order 10^8 M$_\odot$.

The effect of the presence of a secondary BH is not limited to the velocity distribution of ejected stars. Actually, also the branching ratios of ejected stars, i.e. the probability that the system BHB–GC loses stars, depend on the mass ratio ν. Fig. 2 shows the branching ratios for the case of single and binary BH (solid line). In the case of single BH ($\nu = 0$), the branching ratio is 0.267 for the set of parameter studied in this work. For sufficiently low values of the mass ratio, $\nu \lesssim 1/20$, the branching ratio remains nearly constant, while, for higher values, it is an increasing function of ν. Therefore, only if the mass ratio is sufficiently high, the ejection probability in the BHB case increases with respect to the single BH case.

In conclusion, the effect of the binariety, at least when $\nu \gtrsim 1/20$, is dual. Actually, it contemporary enhances the probability of stars ejection, and produces a considerably extended tail in the velocity distribution, corresponding to the production of HVSs.

3.2 The role of the BHB eccentricity

In order to explore the role of the BHB orbital eccentricity, η, we performed, in the case of mass ratio $\nu = 1/4$, a set of simulations for various values of η, $\eta = (0.25, 0.50, 0.75)$. The orbital angular momentum is chosen such that, as in the case of the GC motion, the energy of the BHB elliptical orbits is equal to the energy of the reference circular orbit ($\eta = 0$) of radius $a_h = 0.78$ pc. The

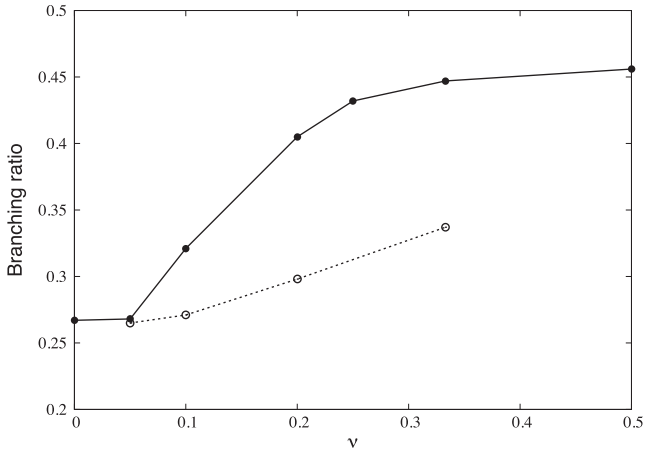

Figure 2. Branching ratios for high-velocity stars as function of the binary mass ratio, ν, for GC orbit coplanar to the BHB orbit (solid line) and perpendicular to it (dotted line).

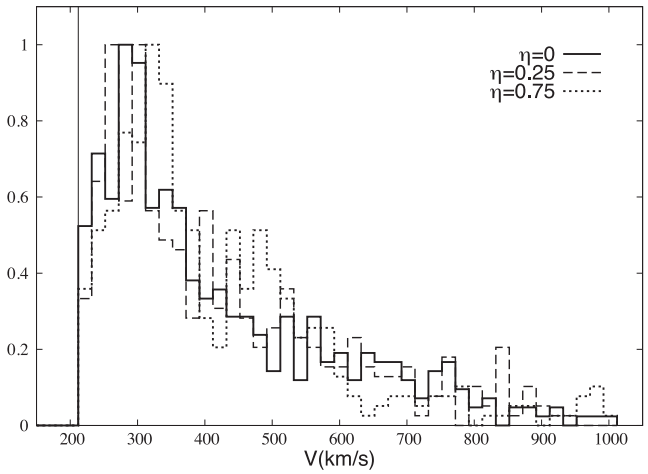

Figure 3. Comparison among the velocity distributions of escaping stars for an SMBHB with mass ratio $\nu = 1/4$ and different eccentricities ($\eta = 0$, 0.25, 0.75). The distributions are cut on the left side at 212 km s^{-1}, which corresponds to the escape velocity from the system evaluated at 20 pc.

initial conditions, assuming that the BHs start their motion at the apocentre, are

$$r_{\rm BH,1} = (1+\eta) r_{\rm BH,1,c}; \quad v_1 = \sqrt{\frac{1-\eta}{1+\eta}} v_{\rm BH,1,c}, \tag{10}$$

for the heavier BH of mass $m_{\rm BH,1}$, while for the lighter BH, $m_{\rm BH,2}$,

$$r_{\rm BH,2} = (1+\eta) r_{\rm BH,2,c}; \quad v_2 = \sqrt{\frac{1-\eta}{1+\eta}} v_{\rm BH,2,c}. \tag{11}$$

Finally, the angle ζ between the semimajor axis of the SMBHB and the x-axis of the Cartesian reference frame is randomly generated.

Fig. 3 shows the resulting velocity distributions for a BHB with mass ratio $\nu = 1/4$ and different orbital eccentricities. It is clear that the tail in the velocity distribution is produced independently of η, with velocities up to $\sim$1000 km s^{-1}. However, different eccentricities do not change the shape of the distribution function with respect to the case of the circular orbit. Therefore, these results suggest that the energy exchange between the generic star of the GC and the BHB is almost independent on the eccentricity, depending only on the initial total energy of the binary.

Table 2. The values of the Branching Ratios (BR) for $\nu = 1/4$ and different BHB orbital eccentricities, η.

η	BR
0	0.432
0.25	0.403
0.50	0.440
0.75	0.425

For what regards the branching ratios, Table 2 shows the branching ratios as function of η. From this table, it is clear that the branching ratio remains nearly constant for different eccentricities. Therefore, not only the shape of the velocity distribution is preserved, but also the probability of star ejection.

To conclude, the BHB orbital eccentricity does not affect neither the shape of the velocity distribution nor the branching ratio of ejected stars. Therefore, the main features of the ejected stars depend on the binary mass ratio ν, but not on the binary eccentricity.

3.3 The role of the GC orbital inclination

In our scattering experiments, the GC orbits are coplanar with the BHB orbital plane. This means that the angular momentum of the GC and that of the BHs are aligned. In order to explore the role of the GC orbital inclination, we performed a set of simulations in the extreme case of GC orbits perpendicular with respect to the BHB orbital plane, in the case of mass ratios $\nu = (1/20, 1/10, 1/5, 1/3)$. The results of our scattering experiments reveal that the GC orbital inclination plays an important role both for the branching ratio and the resulting velocity distribution.

Fig. 2 shows the branching ratios for both the coplanar and perpendicular cases. In the perpendicular case, the branching ratios of the ejected stars are reduced. Actually, the angle between the two angular momentum vectors results to have an important role in the output of the scattering experiments, as the relative inclination of the angular momenta of the GC and of the test star has. Therefore, the actual value of the branching ratio comes from a combination of two effects due to the two-mentioned relative inclinations. Calling β and γ the angles between the pairs of (GC, BHB) and (test star, GC), respectively, the higher probabilities are obtained when $\beta \sim 0$ and $\gamma \sim 0$. Finally, when $\nu \lesssim 1/20$, the branching ratio tends to the value of the single BH case, for which β is not defined and consequently only γ has a role in the output.

The effect of the GC orbital inclination is significant also in the velocity distribution of the ejected stars. Fig. 4 shows the velocity distributions of escaping stars both for the coplanar and perpendicular cases, along with the nearly Gaussian velocity distribution of the case of single massive BH. The velocity distribution is nearly Gaussian also in the perpendicular case, with a tail of HVSs. However, the tail is, in the perpendicular case, much lower than in the coplanar one. For continuity, the general efficiency of the high-velocity star and HVS generation should be enclosed in the two limits (maximum for coplanar and minimum for perpendicular orbits). Moreover, the effect of going from coplanar to perpendicular orbits is the same of reducing the mass ratio ν.

3.4 The role of the GC mass

In order to explore the role of the GC mass, we performed a set of simulations with a light GC, $M_{\rm GC} = 10^3$ M$_\odot$, in the case of BHB mass ratios $\nu = (1/20, 1/10, 1/5, 1/3)$.

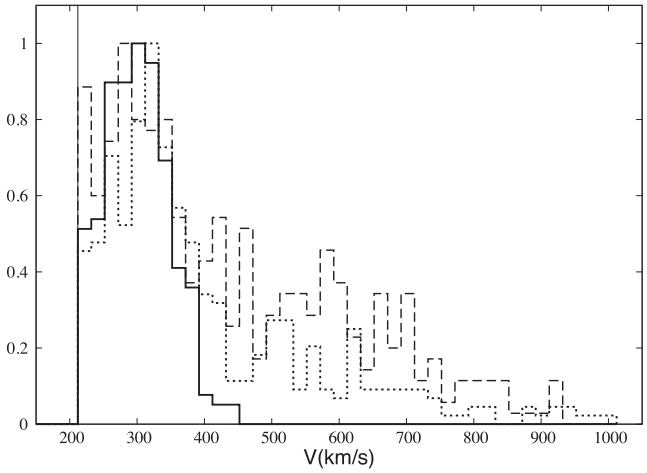

Figure 4. Comparison among the velocity distributions of escaping stars for a single SMBH (solid line) and a binary SMBH with mass ratio $\nu = 1/3$. The dashed line is for GC orbit coplanar to the SMBHB orbital plane, while dotted line is for the case of GC orbit perpendicular to the SMBHB orbit. The distributions are cut on the left side at 212 km s^{-1}, which corresponds to the escape velocity from the system evaluated at 20 pc.

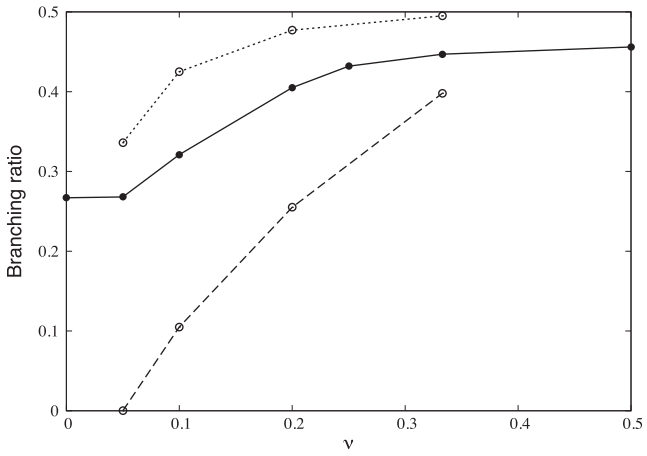

Figure 5. Branching ratios for high-velocity stars as function of the BH binary mass ratio, ν, for $M_{\rm GC} = 10^6$ M$_\odot$ (solid line) and $M_{\rm GC} = 10^3$ M$_\odot$ (dashed line). The dotted line represents the branching ratio for $M_{\rm GC} = 10^6$ M$_\odot$ and a smaller value, $M = 10^7$ M$_\odot$, for the BHB (see Section 3.5).

As expected, the mass of the GC is relevant in the effects of the close interaction with the BHB. Fig. 5 shows the comparison of the branching ratio for $M_{\rm GC} = 10^6$ M$_\odot$ and $M_{\rm GC} = 10^3$ M$_\odot$, as function of the BHB mass ratio ν. The reduction of the GC mass decreases the probability of star ejections. This can be ascribed to two reasons, both linked to the total mass of the cluster (Capuzzo-Dolcetta & Fragione 2015). First, a higher mass implies a stronger gravitational binding of the star to the cluster. Therefore, the cluster is able to carry the star nearer to the BHB and therefore to make the exchange of energy, from gravitational to star kinetic energy, more efficient. On the contrary, a lower cluster mass more unlikely can keep a star bound until the close encounter with the BHB. It may happen, for instance, that the test star is captured by the higher mass BH in the binary, and, as a consequence, it is not accelerated to high velocities. Secondly, the final energy of the star depends also on its initial amount of energy, which is $\propto M_{\rm GC}$; therefore, a

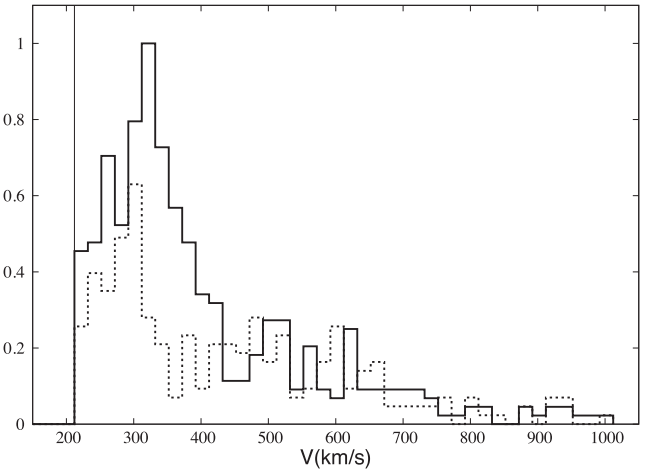

Figure 6. Comparison between the velocity distributions of escaping stars after a $\nu = 1/5$ SMBHB–GC close interaction for $M_{\rm GC} = 10^6$ M$_\odot$ (solid line) and $M_{\rm GC} = 10^3$ M$_\odot$ (dotted line), scaled according to their respective branching ratios. The distributions are cut on the left side at 212 km s^{-1}, which corresponds to the escape velocity from the system evaluated at 20 pc.

lower GC mass means a lower reservoir of energy to convert into kinetic energy when (and if) the star escapes the system.

Fig. 6 shows the velocity distributions of escaping stars, scaled to their respective branching ratios, for the BHB mass ratio $\nu = 1/5$. The two tails are qualitatively similar, although the peak is shifted leftward and downward as effect of the lower GC mass. At the same time, the branching ratio decreases rapidly to $\sim$0 for $\nu \lesssim 1/10$. Therefore, for low BHB mass ratios the probability of ejecting stars at high velocities for low GC mass is negligible. Actually, when $\nu \lesssim 1/10$ the scattering is essentially a three-body interaction among the star, the GC and the heavier BH. As consequence, the probability for star ejection decreases to $\sim$0 because of the low GC mass as already shown by Capuzzo-Dolcetta & Fragione (2015).

Summarizing, the overall effect of reducing the GC mass is that of reducing the probability of star ejection, in particular for low values of the BHB mass ratio.

3.5 The role of the total BHB mass

To explore the role of the total BHB mass, we performed a set of simulations with $M = 10^7$ M$_\odot$, for the mass ratios $\nu = (1/20, 1/10, 1/5, 1/3)$.

As expected the lower mass has a huge effect on the velocity distribution of ejected stars, as shown in Fig. 7. Actually, the lower mass of the BHB leads to a softer interaction with the GC stars and, therefore, to lower ejection velocities. Fig. 7 shows that the peak of the distribution moves to a lower value (the cut is at 67 km s^{-1}, which corresponds to the escape velocity from the system, evaluated at 20 pc, for a GC mass $M_{\rm GC} = 10^6$ M$_\odot$). Moreover, while a tail of high-velocity stars is still present for the lower BHB mass, it constitutes a small fraction of the total escaping stars. At the same time, the branching ratio is slightly higher than in the case of the larger, $M = 10^8$ M$_\odot$, BHB mass for the set of parameters studied in this paper (Fig. 5). The qualitative explanation of this is that, being the radius of the circular GC orbit of reference the same, also the GC pericentres and apocentres remains the same at varying the parameter α. The speed at these points is

$$v_\pm = \frac{\sqrt{\alpha} L_{\rm c}}{r_\pm}, \qquad (12)$$

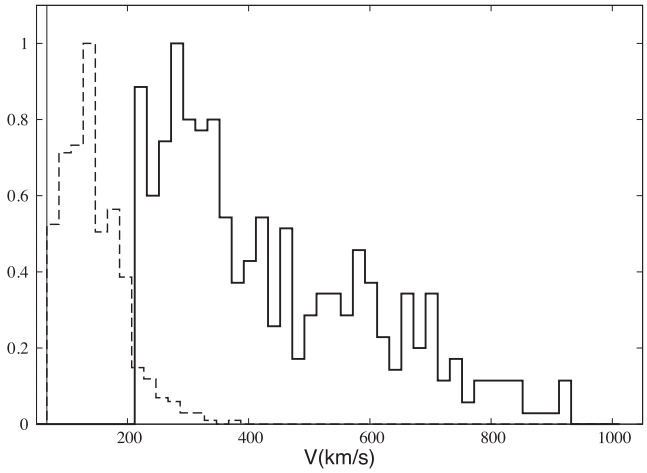

Figure 7. Comparison between the velocity distributions of escaping stars after a $\nu = 1/3$ SMBHB–GC close interaction for $M = 10^8$ M$_\odot$ (solid line) and $M_{\rm GC} = 10^7$ M$_\odot$ (dashed line). The velocity distributions are cut at 212 and 67 km s^{-1}, which correspond to the escape velocities from the system evaluated at 20 pc for $M = 10^8$ M$_\odot$ and $M_{\rm GC} = 10^7$ M$_\odot$, respectively.

so that $v_\pm \propto M^{1/2}$ because $L_{\rm c}$ depends on the mass of the BHB. This scaling behaviour implies that the GC spends more time near the pericentre of its orbit for lower BHB total mass and, consequently, the probability of efficient acceleration of GC stars is higher and the branching ratio increases.

To conclude, the effect of decreasing the BHB total mass is, on one side, to slightly enhance the production of high-velocity stars, while, on the other side, their velocity distribution moves to lower values with respect to the higher BHB mass case, resulting in a negligible tail of high-velocity stars. As consequence, HVSs are not expected to be produced in huge quantity for low BHB masses.

3.6 On the ejection of GCs and light BHs

An interesting result we got from our scattering experiments is that, for some values of involved parameters, the GC was ejected as consequence of the strong interaction with the BHB. This suggests that high-velocity clusters, as, for instance, the one found by Caldwell et al. (2014), may be originated in such a way. This hypothesis deserves, of course, a confirmation by an accurate full N-body modelling.

Studying the effect of the BHB total mass, we investigated also the case $M = 10^6$ M$_\odot$. In this case, we noted that, after some interactions, the lighter BH in the pair was ejected from the system. An intriguing possibility is that such interaction may be the cause of the lack of lighter BH companions for Sgr A*.

4 CONCLUSIONS

The existence of high-velocity stars (Silva & Napiwotzki 2011) has been explained thanks to dynamical ejection mechanisms (Poveda et al. 1967; Gvaramadze, Gualandris & Portegies Zwart 2009) or a supernova ejection mechanism (Blaauw 1961; Portegies Zwart 2000), which are both able to accelerate stars up to several hundreds km s^{-1}. On the other hand, HVSs (Hills 1988) require the presence of a massive BH, or a massive BH binary, due to their extreme velocities, up to thousands km s^{-1} (Yu & Tremaine 2003; Brown 2015).

In this paper, we extended the recent Capuzzo-Dolcetta & Fragione (2015) study, referred to the case of a single BH (Arca-Sedda, Capuzzo-Dolcetta & Spera 2016). Here, we generalize this study to the ejection of high-velocity stars as caused by the close passage of a massive GC near a massive BHB. In the frame of the Λcold dark matter cosmological model, SMBHBs are a natural consequence of the hierarchical paradigm (Begelman et al. 1980; Volonteri et al. 2003). Actually, galaxies may experience multiple mergers during their lifetime and, if more than one of them hosts a massive BH, the formation of a BHB is a natural result.

In our study, we assumed a total mass $M = 10^8$ M$_\odot$ of the SMBHB to have a direct comparison with previous scattering experiments with a single BH of same mass (Capuzzo-Dolcetta & Fragione 2015). The underlying mechanism is a four-body interaction, where the bodies are the SMBHB, the GC (assumed point-like of mass 10^6 M$_\odot$), and a generic test star (1 M$_\odot$) belonging to the cluster. We performed a series of high-precision scattering experiments in order to investigate the probability of ejection of the test star after a close interaction with the SMBHB, and to obtain the velocity distribution of the ejected stars.

Results of Capuzzo-Dolcetta & Fragione (2015) indicated that the test stars velocity distribution after encounters was a narrow nearly Gaussian function, peaked at low values of velocity in dependence on the GC core radius. The ejection velocity was essentially determined by the initial amount of star gravitational energy, $E_{g,*}$, and by the pericentre distance, r_p, of the GC orbit, while the dispersion of the velocity distribution reflects the different initial conditions and the different relative inclination angle between the angular momentum of the cluster orbital motion and that of the test star spinning around the GC. Moreover, when the interaction is with an SMBHB, GC stars feel the additional effect of gravitational slingshots, which enhance their ejection velocity and produce a tail in the velocity distribution, whose extension mainly depends upon the mass ratio, ν, of the BHB components. Actually, the larger the mass ratio, the more extended the distribution towards high velocities. Also the branching ratio for ejected stars depends on the mass ratio ν. Actually, while for low values of ν the branching ratio remains at about the same value (0.27) of the single BH case of mass equal to the total BHB mass, we note that for $\nu \gtrsim 1/20$ the branching ratio is an increasing function of ν.

The same set of simulations made in the case of a BHB of mass ratio $\nu = 1/4$ initially revolving circularly around the centre of mass has been done assuming different orbital eccentricities, η. The shape of the velocity distribution and the values of the branching ratios show that the eccentricity has not a substantial effect on the results. Therefore, the features of the ejected stars depend almost exclusively on the binary mass ratio.

Moreover, we studied the effect of the GC orbital inclination, the GC mass and the BHB total mass. While the overall effect of high GC orbital inclinations and of low GC masses is the reduction of the probability of star ejections, a lower BHB total mass makes the velocity distribution have the peak at lower values, with a negligible tail of high-velocity stars and HVSs.

Finally, it may be relevant noting that GCs are likely mass-segregated, and so more massive stars should move in inner GC regions. The results of this paper would, consequently, imply a dependence on mass of the high-velocity stars. This has some relation with the segregation effects discussed in Perets & Mastrobuono-Battisti (2014) when dealing with nuclear stellar cluster formation around massive BHs in galactic nuclei.

In conclusion, the effect of the binariety, at least when $\nu \gtrsim 1/20$, is dual, because it enhances the probability of stars ejections and

produces an extended tail in the velocity distribution, yielding to the production of HVSs. As a consequence, the infall of various GCs on an SMBHB may enhance the orbital energy loss by the BHB and lead them to the final stage where the main mechanism of the residual energy loss of the binary is gravitational wave emission.

ACKNOWLEDGEMENTS

We thank S. Mikkola for making available to us his ARW code and for useful discussions about his use. Finally, we thank the anonymous referee for useful suggestions and comments about the paper.

REFERENCES

Antonini F., 2013, ApJ, 763, 62
Arca-Sedda M., Capuzzo-Dolcetta R., Spera M., 2016, MNRAS, 456, 2457
Begelman M. C., Blandford R. D., Rees M. J., 1980, Nature, 287, 307
Blaauw A., 1961, Bull. Astron. Inst. Neth., 15, 265
Bromley B. C., Kenyon S. J., Geller M. J., Barcikowski E., Brown W. R., Kurtz M. J., 2006, ApJ, 653, 1194
Brown W. R., 2015, ARA&A, 53, 15
Brown W. R., Geller M. J., Kenyon S. J., Kurtz M. J., 2005, ApJ, 622, L33
Brown W. R. Anderson J., Gnedin O. Y., Bond H. E., Geller M. J., Kenyon S. J., Livio M., 2010, ApJ, 719, L23
Brown W. R., Geller M. J., Kenyon S. J., 2014, ApJ, 787, 89
Bulirsch R., Stoer J., 1966, Numer. Math., 8, 1
Caldwell N., Strader J., Romanowsky A. J., Brodie J. P., Moore B., Diemand J., Martizzi D., 2014, ApJ, 787, L11
Capuzzo-Dolcetta R., 1993, ApJ, 415, 616
Capuzzo-Dolcetta R., Fragione G., 2015, MNRAS, 454, 2677
Capuzzo-Dolcetta R., Miocchi P., 2008, MNRAS, 388, L69
Carollo C. M., Stiavelli M., de Zeeuw P. T., Mack J., 1997, AJ, 114, 2366
Chandrasekhar S., 1943, AJ, 97, 255
Côté P. et al., 2006, ApJS, 165, 57
Fujita Y., 2009, ApJ, 691, 1050
Ginsburg I., Loeb A., 2006, MNRAS, 368, 221
Gnedin O. Y., Gould A., Miralda-Escudé J., Zentner A. R., 2005, ApJ, 634, 344
Gvaramadze V. V., Gualandris A., Portegies Zwart S. F., 2009, MNRAS, 396, 570
Hellström C., Mikkola S., 2010, Celest. Mech. Dyn. Astron., 106, 143
Hills J. G., 1988, Nature, 331, 687
Hoogerwerf R., de Bruijne J. H. J., de Zeeuw P. T., 2001, A&A, 365, 49
Humason M. L., Zwicky F., 1947, ApJ, 105, 85
Kormendy J., Ho L. C., 2013, ARA&A, 51, 511
Loose H. H., Kruegel E., Tutukov A., 1982, A&A, 105, 342
Lu Y., Zhang F., Yu Q., 2010, ApJ, 709, 1356
Marconi A., Hunt L. K., 2003, ApJ, 589, L21
Mayer L., Kazantzidis S., Madau P., Colpi M., Quinn T., Wadsley J., 2007, Science, 316, 1874
Merritt D., Milosavljević M., 2005, Living Rev. Relativ., 8, 8
Mikkola S., Aarseth S., 2001, Celest. Mech. Dyn. Astron., 84, 343
Mikkola S., Merritt D., 2006, MNRAS, 372, 219
Mikkola S., Merritt D., 2008, AJ, 135, 2398
Mikkola S., Tanikawa K., 1999a, Celest. Mech. Dyn. Astron., 74, 287
Mikkola S., Tanikawa K., 1999b, MNRAS, 310, 745
O'Leary R. M., Loeb A., 2008, MNRAS, 383, 86
Palladino L. E., Schlesinger K. J., Holley-Bockelmann K., Allende Prieto C., Beers T. C. Lee Y. S., Schneider D. P., 2014, ApJ, 780, 7
Perets H. B., Alexander T., 2008, ApJ, 677, 146
Perets H. B., Mastrobuono-Battisti A., 2014, ApJ, 784, L44
Perets H. B., Subr L., 2012, ApJ, 751, 133
Perets H. B., Hopman C., Alexander T., 2007, ApJ, 656, 709
Perets H. B., Wu X., Zhao H. S., Famaey B., Gentile G., Alexander T., 2009, ApJ, 697, 2096
Peters P. C., 1964, Phys. Rev. B, 136, 1224
Plummer H. C., 1911, MNRAS, 71, 140
Portegies Zwart S. F., 2000, ApJ, 544, 437
Poveda A., Ruiz J., Allen C., 1967, Bol. Obs. Tonantzintla Tacubaya, 4, 86
Quinlan G. D., 1996, New Astron., 1, 35
Roškar R., Fiacconi D., Mayer L., Kazantzidis S., Quinn T. R., Wadsley J., 2015, MNRAS, 449, 494
Schinnerer E., Böker T., Emsellem E., Lisenfeld U., 2006, ApJ, 649, 181
Schinnerer E., Böker T., Meier D. S., Calzetti D., 2008, ApJ, 684, 21
Sesana A., Haardt F., Madau P., 2006, ApJ, 651, 392
Silva M. D. V., Napiwotzki R., 2011, MNRAS, 411, 2596
Tremaine S. D., Ostriker J. P., Spitzer L. J., 1975, ApJ, 196, 407
Turner M. L., Côté P., Ferrarese L., Jordán A., Blakeslee J. P., Mei S., Peng E. W., West M. J., 2012, ApJS, 203, 5
Volonteri M., Haardt F., Madau P., 2003, ApJ, 582, 559
Yu Q., 2002, MNRAS, 331, 935
Yu Q., Madau P., 2007, MNRAS, 379, 1293
Yu Q., Tremaine S., 2003, ApJ, 599, 1129
Zhang F., Lu Y., Yu Q., 2010, ApJ, 722, 1744
Zhong J. et al., 2014, ApJ, 789, L2
Zubovas K., Wynn G. A., Gualandris A., 2013, ApJ, 771, 118

This paper has been typeset from a TEX/LATEX file prepared by the author.